2022

Comparative Investigation of Structure and Operating Parameters on the Performance and Reaction Dynamic of CO Conversion on Silica Aerogel and Fumed-Silica-Supported Pd Catalysts

Rola Mohammad Al Soubaihi
KTH Royal Institute of Technology

Khaled M. Saoud
Virginia Commonwealth University, s2kmsaou@vcu.edu

Joydeep Dutta
KTH Royal Institute of Technology

Surfaces and Interfaces 29 (2022) 101776

Contents lists available at ScienceDirect

Surfaces and Interfaces

journal homepage: www.sciencedirect.com/journal/surfaces-and-interfaces

Comparative investigation of structure and operating parameters on the performance and reaction dynamic of CO conversion on silica aerogel and fumed-silica-supported Pd catalysts

Rola Mohammad Al Soubaihi [a], Khaled Mohammad Saoud [b], Joydeep Dutta [a,*]

[a] Functional Materials, Department of Applied Physics, KTH Royal Institute of Technology, Hannes Alfvéns väg 12, 114 19 Stockholm, Sweden
[b] Virginia Commonwealth University in Qatar, Liberal Arts and Sciences Program, P.O. Box 8095, Doha, Qatar

ARTICLE INFO

Keywords:
CO oxidation
Hysteresis
Thermal stability
Pretreatment
Structure-activity
Sol-gel
Supercritical drying

ABSTRACT

The catalyst morphology, metal-support interaction, and reaction conditions greatly influence the catalytic performance and reaction dynamics. Similarly, the dispersion of the metal within the support plays a crucial role in the thermal stability and sintering of the catalyst. Furthermore, temperature-dependent conversion hysteresis is well-known to occur during ignition and extinction of exothermic CO oxidation over supported Pd catalysts due to the variation of CO adsorption on the surface or bulk oxidation of Pd and the ability of the catalyst to regenerate the active sites. Herein, the catalytic performance and the hysteresis behavior of mesoporous silica aerogel supported Pd (Pd/a-SiO_2), and commercial fumed silica-supported Pd (Pd/f-SiO_2) were investigated and compared using CO oxidation as a probe reaction under different reaction conditions and operating parameters (i.e., catalyst weight, ramp rate, and flow rate). Surface and morphologic examination using XPS, FTIR, and TEM of Pd/a-SiO_2 and Pd/f-SiO_2 reveal a strong correlation between the catalyst surface and structure and its catalytic performance and stability under different reaction parameters. Moreover, this study presents the effect of surface area, particle size, and size distribution on diffusion and mass transport of reactants (CO, O_2) and products (CO_2) and active sites accessibility.

This study showed that Pd/f-SiO_2 had better efficiency under high (turbulence) flow. Moreover, intrinsic apparent activation energy (E_a) and the number of active sites were calculated from the Kinetics of CO oxidation fitted using Arrhenius plots indicate that the ramp rate has less effect on Pd/f-SiO_2 catalytic behavior. Even though, Pd/f-SiO_2 had higher relative active sites than Pd/a-SiO_2, (E_a) was lower. Cyclic stability and long-term stabilities showed that both catalysts are stable and can regenerate the active sites. The current study contributes to understanding the catalysts' surface, structural and morphological properties on the catalysts' performance toward CO oxidation and other reactions under dynamic conditions.

1. Introduction

CO oxidation reaction has attracted significant attention, and it is considered a crucial reaction today in the field of heterogeneous catalysis, primarily due to its significant applications in the automotive industry and the protection of environmental contamination [1]. Noble metals (Pt, Pd, Au, etc.) [2], base metals (Cu, Mn, Co, Fe, etc.) [1,3,4], and metal alloys [5] have been used as a low-temperature catalyst for CO oxidation with enhanced catalytic activity. Pd stands out as a catalyst of choice for many applications due to its high intrinsic activity. Pd catalysts are considered crucial for many reactions and used as a model reaction for studying catalyst structure-activity relationship, metal-support interaction, and other nonlinear dynamic behavior during CO oxidation [6–8]. However, Pd catalysts' properties are susceptible to preparation and operation conditions, i.e., the nature of support and dispersion of the Pd nanoparticles within the support matrix influences its activities [9]. Catalyst support materials play a crucial role in the catalytic activity and catalytic behavior of the Pd catalyst, where the nature of supports influences the synergistic effect between Pd and the supports. Pre-treatment conditions can induce the formation of oxygen vacancies and hydroxyl groups around Pd particles or on the support's surface, facilitating Pd dispersion and influencing the electronic structure of the active sites for CO oxidation [10]. Silica supports are used for anchoring and dispersing metal nanoparticles on the functional silica

* Corresponding author.
E-mail address: joydeep@kth.se (J. Dutta).

https://doi.org/10.1016/j.surfin.2022.101776
Received 8 November 2021; Received in revised form 26 December 2021; Accepted 29 January 2022
Available online 4 February 2022

surfaces [11], high surface area and tunable surface properties, good thermal stability, and varied morphologies [12]. Aerogel [7], mesoporous silica [13], rods, etc., have been widely explored also for CO oxidation [14,15].

Silica aerogels with high porosity consist of a silica network and have been used in many catalyzed reactions [9], wherein the aerogels were reported to show enhanced catalytic activity due to local heating and heat retention properties [10,14]. Fumed silica is used as a raw material for additives in various chemical industry products [16,17]. Fumed silica could be promising catalyst support due to its lower cost, small particle sizes, and high surface area. For example, Kang *et al.* reported the synthesis of sustainable heterogeneous fumed silica-supported Pd nanocatalyst for Suzuki-Miyaura reactions with good recycling properties [18].

Pd catalysts can exhibit nonlinear dynamics under oxidizing conditions such as hysteresis, as observed in different heterogeneous catalytic reactions. Hysteresis is a common phenomenon in the oxidation of CO [19] that has been reported for many oxidation reactions on noble metal catalysts [6,20] and attributed to noble metal oxidation [21] or overheating of the active site [22]. Reaction exotherm and the interplay between kinetics and mass transfer play a crucial role in the hysteresis phenomenon. The diffusion resistance and total mass transfer effects on the CO conversion hysteresis were reported and attributed to gas propagation through the catalyst bed and the catalyst structure [23].

To the best of our knowledge, there are very few reports on the effect of operation parameters on the catalytic activity and the hysteresis phenomenon during ignition/extinction CO oxidation. Recently, we reported the synthesis, effect of porosity, and preparation conditions on the catalytic properties and hysteresis behavior of the Pd/a-SiO_2 catalyst. In this work, we compare the CO catalytic performance, and the occurrence of hysteresis effects in the CO oxidation reaction over silica aerogel supported palladium (Pd/a-SiO_2) and commercial fumed silica-supported palladium (Pd/f-SiO_2). Furthermore, we investigate the effect of catalyst's structure (i.e., type of silica support) and operation parameters (i.e., catalyst weight (mass), flow rate, weight hourly space velocity, and ramp rate) on the catalytic CO conversion, hysteresis behavior, and stability of both under controlled conditions and as a function of catalyst temperature. This study contributes to a better understanding of catalyst structure and operation conditions on the catalytic performance, dynamic hysteresis, and CO oxidation stability, which can aid chemical reactions using these catalysts.

2. Experimental methodology

2.1. Catalyst preparation and characterization

Pd/a-SiO_2 catalyst was prepared using the sol-gel technique using tetraethyl orthosilicate (TEOS) and ethanol as starting materials, as explained in details elsewhere [24], dried under conditions with supercritical ethanol at 260 ° C. The Pd precursor (palladium chloride ($PdCl_2$), Sigma-Aldrich) was impregnated during the gelation step before the drying step to achieve a good dispersion of Pd particles on the silica aerogel support, which is achieved by replacing the solvent inside the pores with Pd precursor [7]. The synthesized Pd/a-SiO_2 catalyst ensures that the palladium particles are located inside the pores or within the silica particulate network with a very small agglomeration of Pd particles [25]. Dried Pd/a-SiO_2 aerogels were then removed from the autoclave and calcinated by annealing at 450 °C (heating rate of 10 °C) under atmospheric pressure (1 atm) in ambient conditions. The Pd/f-SiO_2 catalyst was prepared using the deposition preparation method (DP), where the Pd precursor was introduced onto the f-SiO_2 support [26]. In a typical synthesis procedure, a chosen amount of anhydrous $PdCl_2$ was first dissolved in 10 mL of ethanol to obtain a solution of Pd wt% corresponding to a (5% wt.) Pd loading. The solution was added drop-wise to 1 g of fumed silica (Nanonext Ltd, UK) under continuous stirring in distilled water for 1 h. 15 ml 2 M NaOH solution was added drop-wise to this solution until the pH became neutral. The solution was subjected to another 30 min of continuous stirring. The resultant Pd/f-SiO_2 catalyst was filtered, washed several times with DI water and ethanol, then dried at 105 °C in an atmospheric oven for 1 h, then calcination in air at 450 °C for another hour. Surface area and porosity analyzer Rise 1010 (Jinan Rise Science and Technology Co., Ltd., China) was utilized and nitrogen adsorption-desorption isotherms were recorded at 77 K using the multiple-point BET method in the relative pressure range of P/P0 = 0.05–0.2 and fitted based on Brunauer–Emmett–Teller (BET) and Langmuir models. Inductively coupled plasma–optical emission spectroscopy (ICP-OES) (iCAP 6000 series, Thermo Scientific) was used to measure the amount of palladium in the catalyst samples. X-ray diffraction (XRD) (X'Pert PRO X-ray diffractometer, USA) to study the crystallography, X-ray photoelectron spectroscopy (XPS; Omicron Nanotechnology, Germany) to study the surface states of the catalyst. XPS data were calibrated using the C 1 s located at 285 eV as a reference [27]; transmission electron microscopy (TEM) measurements were carried out using a (JEM2100F field emission transmission electron microscope (TEM), JEOL Ltd., Japan). Fourier transform infrared (FTIR) spectroscopy and FTIR650 Spectrometer with LA-025–1100 universal ATR unit (Labfreez Instruments (Hunan) Co., Ltd., Hunan, China).

2.2. Catalyst activity testing

The catalytic activities of the synthesized samples were carried out following a procedure described elsewhere [7]. In a typical test, a custom-built fixed-bed continuous flow reactor placed inside a tube furnace connected to an infrared gas analyzer (ACS- CO_2 Infrared analyzer), a 20 mg of powdered metal loaded aerogel catalyst was placed in the middle of the quartz tube and sandwiched between two pieces of glass wool to form a cylindrical pallet. The catalyst temperature was recorded using Omega K-type thermocouple inserted in the middle of the catalyst. A reactant gas mixture containing 3.50 wt% CO and 20.0 wt% O_2 balanced with helium was flown through the catalyst bed at a 100 cm^3/min flow rate. The CO oxidation reaction was performed by changing the catalyst mass, flow rate, heating rate, keeping the catalyst bed diameter and length at 10 mm and 2 mm, and fixed gas hourly space velocity (GHSV) of the feed gas mixture at 38,200 h^{-1}. Temperature and the concentration data were collected using the National Instruments data acquisition board and recorded using a custom-built LabVIEW data acquisition program. The gas flow rate was controlled by digital mass flow controllers. The flow rate of the mixture was maintained at 100 mL/ min while the catalyst was heated to different temperatures (35 °C–600 °C) and atmospheric pressure (1 atm) with a heating rate of 10 °C/min (Ignition or activation) until the CO conversion reached 100% conversion when the samples were left to cool naturally under a continuous flow of the gas mixture until the CO conversion reaches (0%) (extinction or relaxation). The samples were calcinated at 450 °C in air for 1 h before the catalytic activity test to reduce the metal precursor and remove moisture and adsorbed impurities. Ignition (light-off) and extinction (light-out) temperatures are the temperatures where the concentration of CO_2 is 3% during heating and cooling cycles [28]. In the present study, we define the ignition-extinction hysteresis as (ΔT_{50}= $T_{50\text{-}h}$- $T_{50\text{-}c}$); the difference between the catalyst (reaction) temperature at which the CO conversion efficiency reaches 50% during ignition ($T_{50\text{-}h}$) and the temperature at which the CO conversion efficiency reaches 50% during extinction ($T_{50\text{-}c}$).

3. Results and discussions

BET surface area of Pd/a-SiO_2 was ~x223C1114 m^2/g, while the surface area of Pd/f-SiO_2 was ~x223C287 m^2/g. ICP-OES analysis of Pd/a-SiO_2 showed an average concentration of Pd ~x223C162 ppm (± 0.02 ppm), approximately 6.0% of the catalyst mass. On the other hand, Pd/f-

SiO_2 showed an average concentration of Pd ~x223C144 ppm (± 0.02 ppm), approximately 5.3% of the catalyst mass. The crystal structure of both catalysts was identified in XRD spectra, Fig. S1. The samples consist of Pd, SiO_2 phases with a small fraction of PdO noticeable only in Pd/a-SiO_2 as observed from the diffraction line detected at $2\theta = 44.5°$ from PdO (112) plane.

3.1. Catalytic performance of Pd/a-SiO_2 and Pd/f-SiO_2 catalysts at different reaction conditions

3.1.1. Effect of catalyst weight

The ignition and extinction profiles of Pd/a-SiO_2 (Fig. 1(a) and Table S1) vary significantly as the catalyst weight varies. It can be observed that 20 mg of catalysts showed the lowest T_{ig}, highest catalytic activity, and widest hysteresis width (ΔT_{50}). Increasing the catalyst weight increases the number of active sites, thus improving the catalytic CO conversion. Further increase in catalyst weight does not improve the conversion, as reported in other work [29]. These results could be attributed to the resistance to diffusion of reactant species in the catalyst when higher catalyst mass was used, inducing mass transfer limitations in the reaction zone where the competition between the reaction kinetics and diffusion leads to a wider hysteresis curve. These are mainly caused by the heat generated from the exothermic reaction at the ignition zone, which heats the catalyst during the continuous reduction of the inlet gas temperature (below the ignition temperature) [30].

However, Pd/f-SiO_2 catalyst (Fig. 1(b) and Table S1) show different behavior wherein the ignition and extinction profiles increase linearly as the catalyst weight increases. It can be observed that the catalyst weight of 30 mg showed the lowest T_{ig} and highest catalytic activity. Similar results were obtained in previous reports suggesting that increasing catalyst weight increases the catalytic activity for CO oxidation due to the increase in the total surface area and the number of active sites on the catalyst surface that would lead to enhanced CO and O_2 adsorption on the catalyst surface, followed by dissociation of O-O bonds to react with CO, finally forming CO_2 molecules [31]. ΔT_{50} showed a similar trend for Pd/a-SiO_2, where the conversion and hysteresis go through a maximum with increasing catalyst weight. ΔT_{50} at 20 mg catalyst showed the widest CO conversion hysteresis; This behavior is attributed to mass transfer limitations when using high catalyst weight, similar to the explanations above.

3.1.2. Effect of ramp rate

The catalytic activity, hysteresis, and ignition/extinction profile of Pd/a-SiO_2 and Pd/f-SiO_2 catalysts were compared at 5, 10, and 20 °C/min, for a constant catalyst weight of 20 mg and 100 mL/min flow rate, as shown in Table S2 and Fig. 2(a) and (b). The heating rate significantly impacts the catalytic ignition/extinction profile of the Pd/a-SiO_2 catalyst, with the ignition/extinction curve shifted to higher temperatures for higher heating rates. The sample heated at 10 °C/min yielded higher CO conversion at a lower T_{ig} at ~x223C175 °C. All ramp rates showed normal hysteresis. Pd/f-SiO_2 catalyst showed a different behavior, where the ramp rate has less effect on catalytic behavior. The sample heated at 5 °C/min yielded higher CO conversion at a lower ignition temperature of 184 °C, slightly lower than samples heated at 10 °C/min and 20 °C/min. All ramp rates showed normal hysteresis; however, the sample heated at 5 °C/min showed a narrower hysteresis width at 50% conversion.

The behavior in Pd/a-SiO_2 can be attributed to the low reaction rate at the temperature below the T_{ig}, where the reaction is only kinetically controlled. The conversion is controlled by the internal diffusion and mass transfer limitation at a temperature higher than the T_{ig} and lower than the 100% conversion. When the temperature is above T_{50}, the reaction rate is high and controlled by external diffusion with no mass transfer limitation. As a result, a low ramp rate leads to a higher activation energy. The kinetic and reaction rates are high in the higher ramp rate, leading to less collision, higher light-off temperature, and less conversion. In contrast, the case on the fumed silica is different because there is no internal diffusion and mass transfer limitation; the effect of ramping rate is negligible.

These results agree well with previous reports [22,32]; thus, increasing the heating rate increases the thermal energy of gas molecules, enhancing the collision frequency where there is a sufficient molecule with energy higher than the activation energy, which results in faster kinetics and less diffusion.

3.1.3. Effect of flow rate

Table S3 summarizes the catalytic activities and the hysteresis width for both catalysts during the ignition and extinction for different flow rates in 20 mg catalyst at 10 °**C** /min ramp rate. CO conversion activity and the hysteresis width variation of both catalysts become more evident during the extinction curves. For Pd/a-SiO_2 catalyst (Fig. 3(a)), T_{ig}= 175 °C observed at 100 mL/min is the least compared to T_{ig} at 50 mL/min and 200 mL/min. However, $T_{50\text{-}h}$ is less at 200 mL/min.

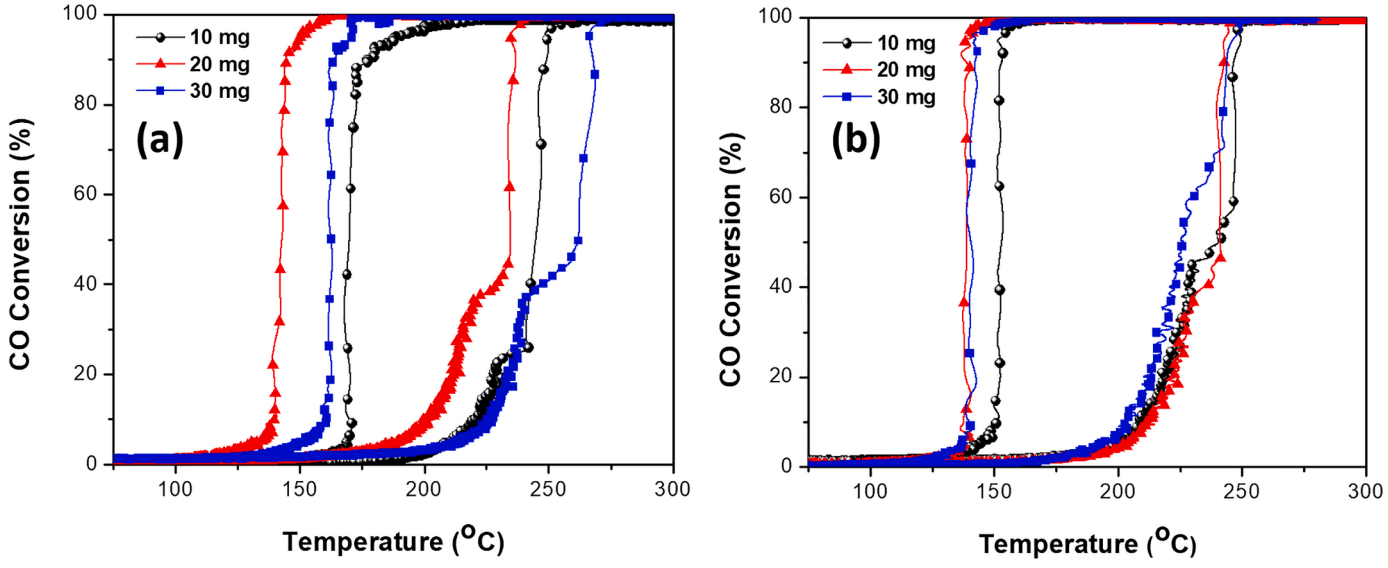

Fig. 1. Catalytic ignition and extinction profiles of Pd/a-SiO_2 aerogel and Pd/f-SiO_2 catalysts at different catalyst weights (mass); 10 mg (black), 20 mg (red), and 30 mg (blue). (For interpretation of the references to color in this figure legend, the reader is referred to the web version of this article.)

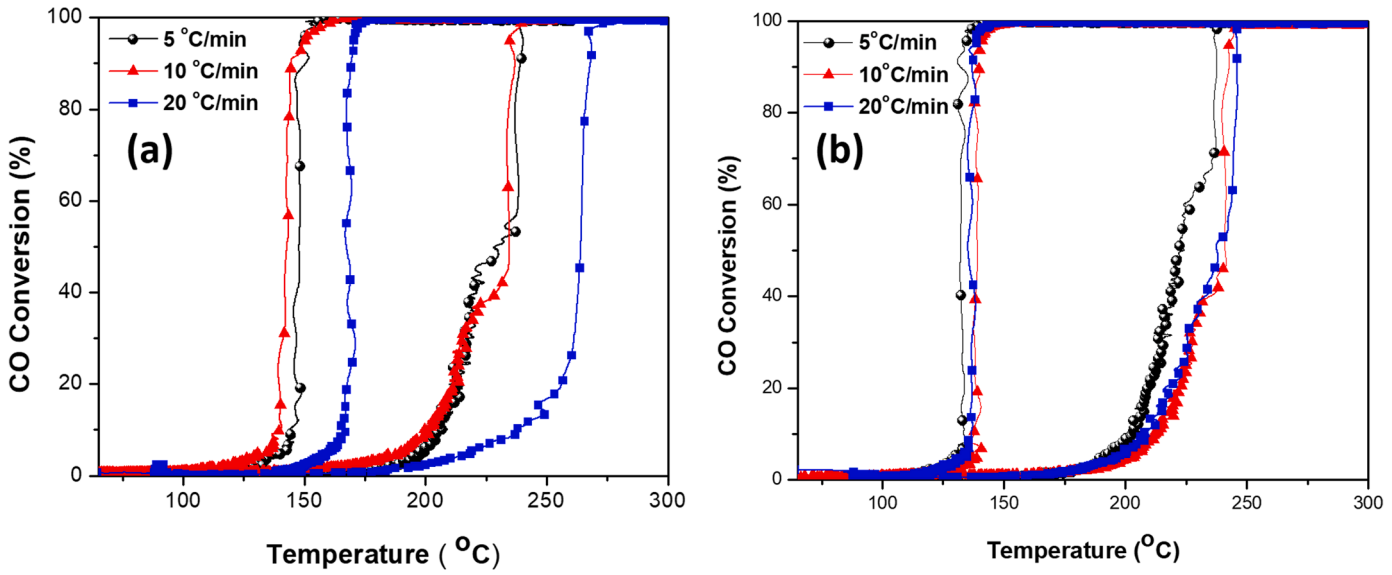

Fig. 2. Catalytic ignition and extinction profiles for a 20 mg catalyst and 100 mL/min flow rate of (a) Pd/a-SiO_2 and (b) Pd/f-SiO_2 catalysts as a function of ramp rate at 5°C/min (black), 10 °C/min (red), and 20 °C/min (blue). (For interpretation of the references to color in this figure legend, the reader is referred to the web version of this article.)

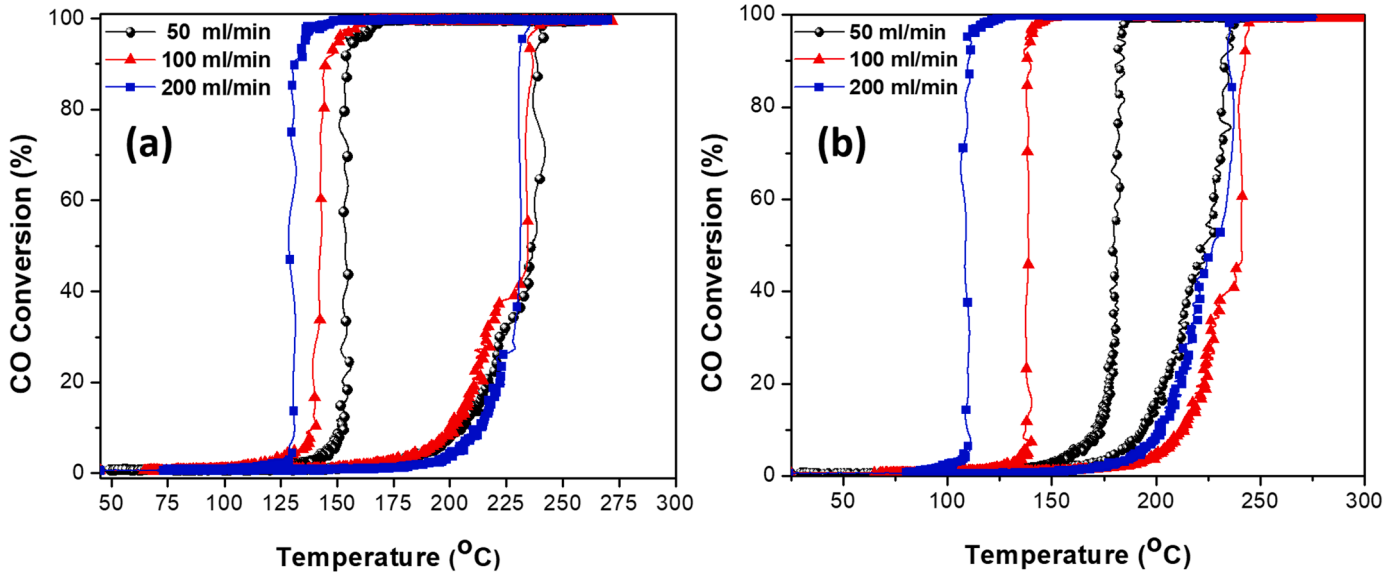

Fig. 3. Catalytic ignition and extinction profiles of (a) Pd/a-SiO_2 and (b) Pd/f-SiO_2 at flow rates 50 ml/min (black), 100 ml/min (red), and 200 ml/min (blue). (For interpretation of the references to color in this figure legend, the reader is referred to the web version of this article.)

Furthermore, hysteresis width ΔT_{50} was slightly increased by 10 °C when the flow rate was doubled. The results suggest that although T_{ig} with 100 mL/min flow of gas is the lowest, the catalytic activities of Pd/a-SiO_2 do not appreciably depend upon flow rates of reactant gas. Fig. 3 (b) shows the CO conversion hysteresis of Pd/f-SiO_2, where 50 mL/min flow seems to be the most optimum, leading to the lowest T_{ig}= 172 °C, $T_{50\text{-}h}$, and T_{100}. Increasing the flow rate reduced the overall activity and caused ignition temperatures to shift to higher temperatures due to reduced contact time and increased mass transport. At higher flow rates, CO conversion showed lower ignition and extinction temperatures at 200 mL/min due to turbulence flow of gas mixture, which leads to better mixing and increases the contact time of reactants compared to the100 mL/min laminar flow that leads to forming of a laminar film on the catalyst surface causing the lower catalytic activity.

During the extinction, increasing the flow rate reduced the $T_{50\text{-}c}$ and increased ΔT_{50}, which increased by ~x223C50 °C when the flow rate was doubled. Increasing flow rate has a more prominent effect on CO conversion hysteresis of Pd/f-SiO_2 than Pd/a-SiO_2, which shows that the changing of flow rate has less effect on the activity of porous catalysts. The widening of hysteresis for increasing flow rates of reactants could be attributed to the isothermal behavior of the catalysts and the external mass transport at higher temperatures. The results show that the changing of flow rate has less effect on the activity of porous catalysts.

TEM, FTIR, XPS were used to explore the morphology of the two catalysts. TEM images of aerogel and fumed silica-containing Pd nanoparticles (Fig. 4) show that the distribution of Pd nanoparticles and morphology are uniform in both samples. However, it can be observed in Fig. 4a that Pd/a-SiO_2 is highly porous and showed finely dispersed small Pd particles with a size (~x223C2–5 nm) located inside the microporous framework of SiO_2 aerogels with a few larger particles

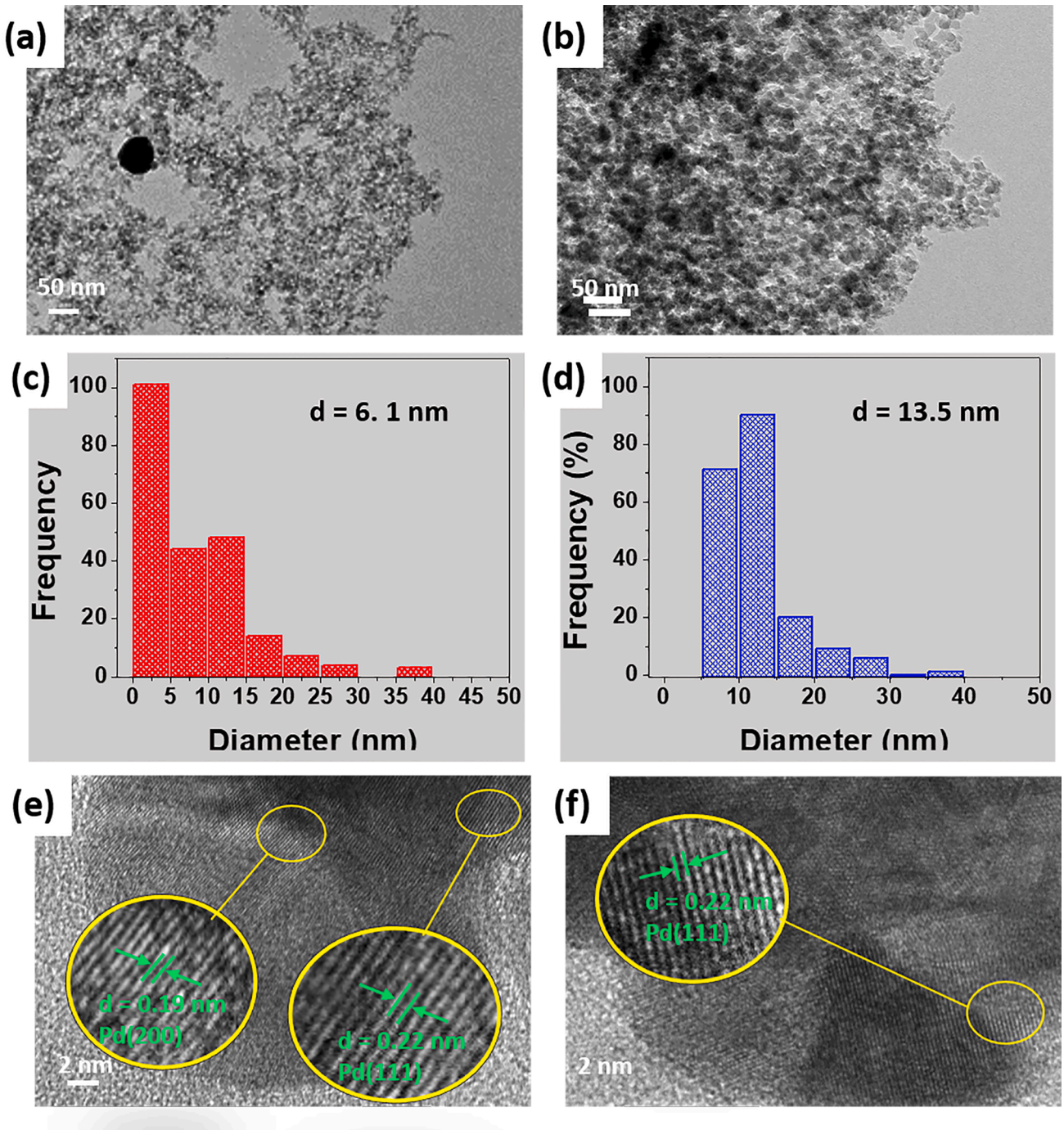

Fig. 4. Transmission electron micrographs (TEM) of fresh Pd/a-SiO_2 (a, c) and Pd/f-SiO_2 (b, d) catalysts.

(~x223C15–35 nm) quite similar to reports in the literature [24,25]. This unique texture is advantageous to the sol-gel synthesis that results in a sinter-proof Pd particle. Pd/f-SiO_2 samples are less porous, and the Pd nanoparticles are (~x223C5–16 nm) but poorly dispersed on the surface of fumed silica, as shown in Fig. 4b. Fourier transform diffraction spectra in the aerogel and fumed silica samples are shown in Fig. 1e and 1f, respectively.

FTIR spectra of samples (Fig. 5) show the presence of a considerable amount of silanol groups on the silica surface or the pores in the Pd/a-SiO_2 sample indicated by the peak centered at 962.3 cm^{-1} corresponds to the stretching vibration of silanol groups (Si-OH) in the silica lattice [33]. Pd/f-SiO_2 catalysts revealed typical silica material peaks at 808 cm^{-1} (with ~x223C13.5 cm^{-1} shift), 1076 cm^{-1} (with ~x223C 23 cm^{-1} shift) corresponding to stretching vibrations of siloxane groups (Si–O–Si bonds). The shift of the Pd/f-SiO_2 sample peaks to a higher wavenumber indicates the interaction between Pd and SiO_2 that can affect the formation of the Si-O-Si network, as observed in Cu/SiO_2 [34]. The absence of the peak centered at 962.3 cm^{-1} indicates that the Pd/f-SiO_2 sample contains no silanol groups (Si-OH).

XPS analysis of Pd 3d was used to investigate the interaction between Pd and the underlying SiO_2 in either sample. Fig. 6 shows Pd 3d of Pd/a-SiO_2, Pd/f-SiO2 catalysts, and their deconvoluted peaks, as in Fig. 6a. Spectral fitting leads to two distinct peaks at binding energy (BE) of 334.1 and 339.7 eV corresponding to metallic Pd in the form of Pd^0, respectively. Two other peaks at BE of 336 eV and 341.2 eV correspond to form Pd^{2+}. BEs of 334.1 and 341 eV correspond to metallic Pd in the

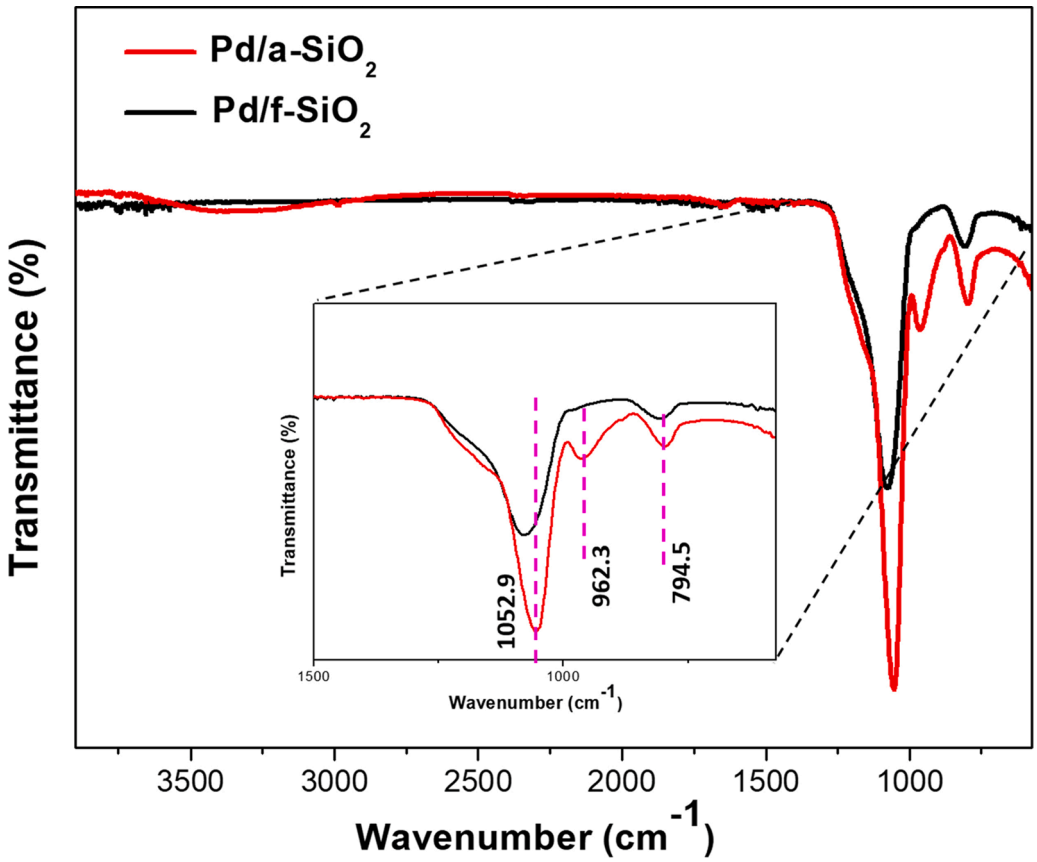

Fig. 5. FTIR spectra of fresh Pd/a-SiO_2 aerogel and Pd/f-SiO_2 catalysts.

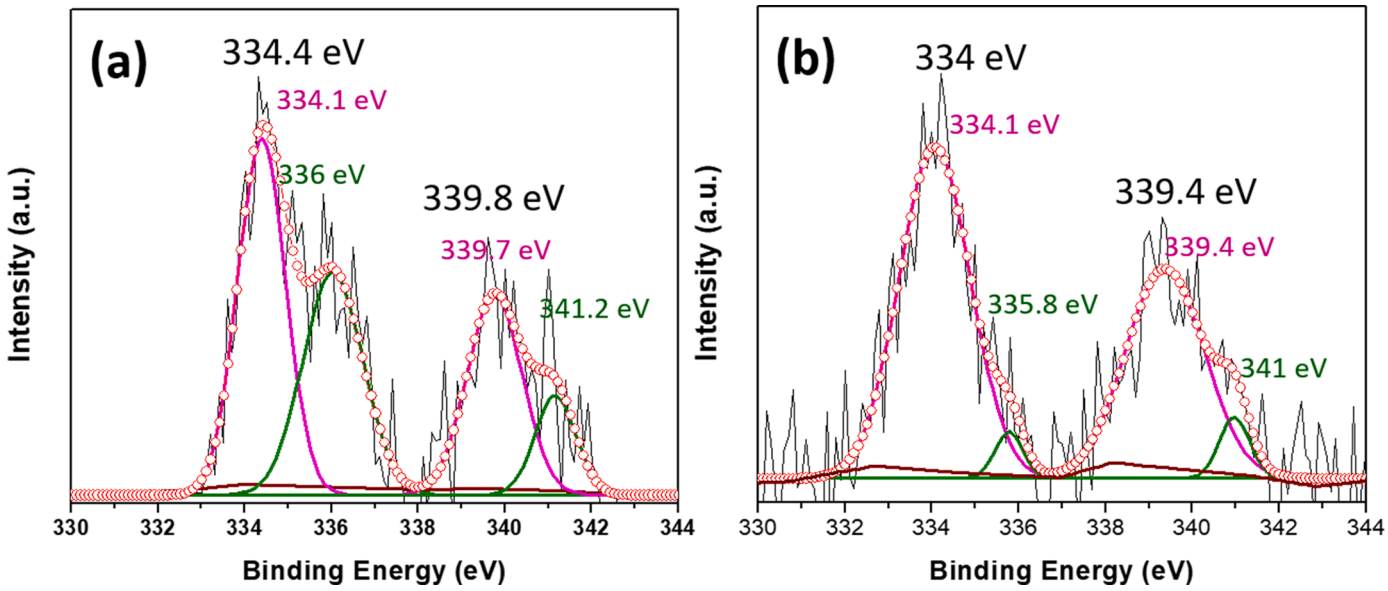

Fig. 6. High-resolution Pd 3d XPS spectrum obtained for fresh (a) Pd/a-SiO_2 and (b) Pd/f-SiO_2 catalysts.

form of Pd^0 and very small peaks of Pd^{2+}. XPS data showed that all the peaks were shifted to slightly lower binding energies, suggesting a strong interaction between the silica support and palladium. This shift indicates an electron transfer from Pd to the silica support [26], thus indicating a strong metal-support interaction at the interface between Pd and Si [35]. These results conform to the XRD studies' observations that Pd and PdO fraction are present in Pd/a-SiO_2 while Pd in its oxidized form does not form in Pd/f-SiO_2.

3.2. *Kinetics of CO oxidation over Pd/a-SiO_2 and Pd/f-SiO_2 catalysts*

The effect of residence time and space velocity on the apparent activation energy of CO oxidation reaction was investigated as a function of the reactant's flow rate. The space velocity corresponds to the reciprocal of the residence time (g s μmol^{-1}), defined as the ratio of the mass of catalyst (W_{cat}) to the molar flow rate of CO at the reactor inlet (F_{CO}). Residence time provides valuable information about the catalytic

activity and activation energy (E_a) for CO oxidation over supported Pd catalysts and is expected to allow obtaining a limiting E_a, which is directly related to the adsorption potential of the active centers [36]. Several studies have reported the flow rate effect on the catalytic activity for oxidation reactions and hysteresis [37,38]. Fig. S2 and Table S4 showed the CO conversion as a function of weight hourly space velocities (WHSV) over Pd/a-SiO2 and Pd/f-SiO2 catalysts under different flow rates.

The CO conversion over 20 mg of Pd/a-SiO_2 and Pd/f-SiO_2 catalysts at different temperatures and flow rates (50, 100, 200, and 400 ml/min) was found by comparing the activation energy (E_a) and the space velocities over the two catalysts.

CO oxidation experiments were performed under differential conditions to collect intrinsic kinetic data in the initial rates range. The reaction rates ($-r_{CO}$) used to obtain the intrinsic activation energy of the Eley–Rideal mechanism of CO oxidation to CO_2 from fractional CO conversion versus residence time (W_{cat} / F_{CO}) data:

$$(-rCO) = \frac{X_{CO}}{W_{cat}/F_{CO}} \quad (1)$$

The apparent activation energies of the catalysts were determined from the Arrhenius plots according to the following equation:

$$Ea = \frac{\mathrm{Ln}\ (r_{CO})}{1/\mathrm{T}} \quad (2)$$

Where X_{CO} is the fractional CO conversion, F_{CO} is the CO flow rate in μmol s^{-1}, W_{cat} is the catalyst weight in g, and ($-r_{CO}$) is the reaction rate in μmol $g^{-1}s^{-1}$. CO conversions were kept well below 15% in kinetic measurements performed under differential conditions and data obtained at different flow rates (50- 400 ml/min).

The apparent activation energy is lower for Pd/a-SiO_2, as shown in Fig. 7(a) and (b). Lower E_a may be attributed to the small particle size shown in the TEM analysis and the high dispersion of Pd in the Pd/a-SiO_2 sample [39]. Furthermore, the calculated relative active sites from the pre-exponential factor in Arrhenius plots in both catalysts are higher in Pd/f-SiO_2 (~x223C252) than Pd/a-SiO_2 (~x223C153).

The results agree with the previous experimental and theoretical analysis [2,40] that the lower inlet gas flow and the higher surface-to-volume ratio will cause the lower E_a.

3.4. Catalyst stability

3.4.1. Cyclic stability of the catalysts

Preparation of the highly stable Pd/a-SiO_2 and Pd/f-SiO_2 catalysts with active sites' regeneration ability under the same reaction conditions is crucial to maintain reliable run-to-run CO conversion. The cyclic stability test can emphasize the influence of reaction conditions on catalytic activity and stability. For this purpose, the catalyst recycles experiments for both catalysts were carried out for four subsequent runs, and the results are shown in Fig. 8. CO conversion was measured as a function of reaction temperature for four consecutive heating and cooling cycles under a continuous flow of CO/O_2 mixture over the catalyst bed without removing the catalyst. After each run, the catalyst was recovered by cooling to room temperature for 1 h, and then the subsequent test was performed wherein even after four cycles of the catalyst usage, no decline of catalytic activity was observed. Fig. 8(a) and (b) show the ignition/ extinction conversion curve as function of time. The four cycles show similar results, which indicate that both catalysts are stable and active sites can be reproduced.

3.4.2. Long-term catalyst stability

The long-term catalytic activity of Pd/a-SiO_2 and Pd/f-SiO_2 catalysts with 5% Pd loading was performed under a continuous flow of gas under specific reaction conditions (3.5% CO, 20% O_2, and 100 ml/min flow rate) until 100% CO conversion to CO_2 was achieved, following which the catalysts were left to cool normally (after turning off the furnace) at 150 °C. The temperature was stabilized at 150 °C (by turning on the furnace) for 27 h. The results show that both catalysts are very stable for long-term usage. It can be concluded from Fig. 8(c) and (d) that both catalysts exhibited high catalytic activity without any decrease in CO conversion and exhibited catalytic stability during the entire 27 h stability test. The catalyst maintains at full conversion without any deactivation during the whole 27 h reaction time on stream

Evaluating the catalytic activity and investigating the hysteresis in humidity is important in any real-life application. The catalytic activity and the hysteresis behavior of both catalysts were investigated in dry conditions (RH =1%) and humid conditions; approximately (RH = 20%) relative humidity and shown in Fig. S3.

4. Conclusions

We compared the CO conversion efficiency and hysteresis behavior

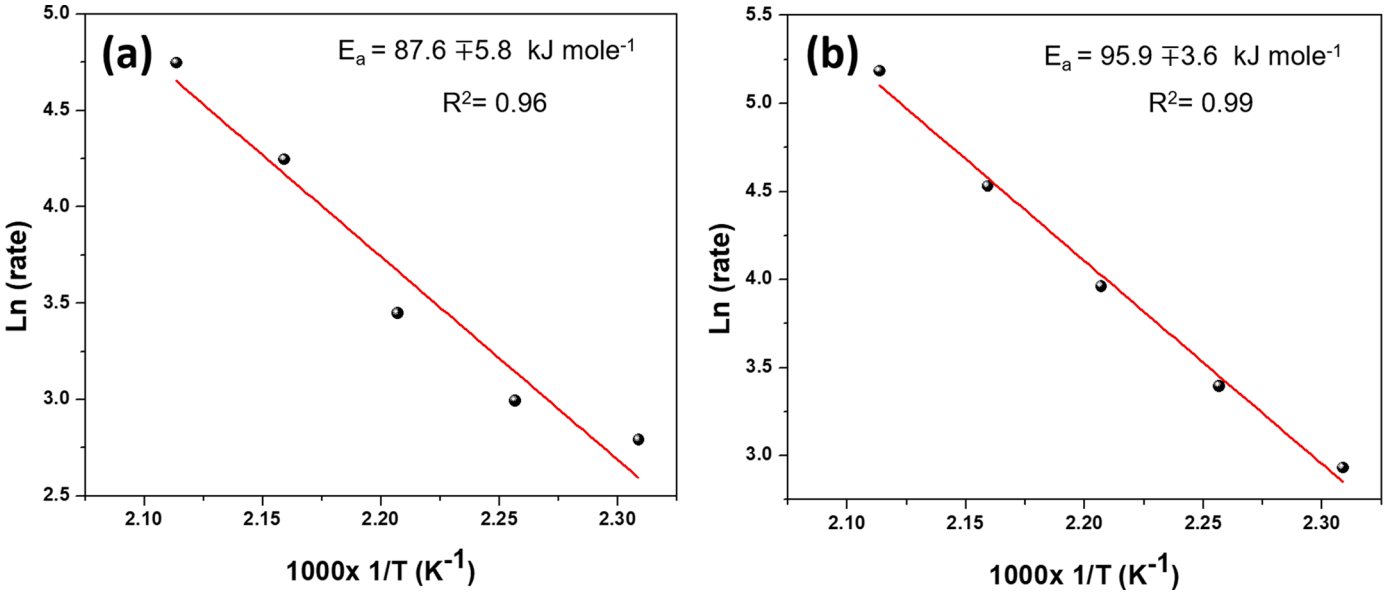

Fig. 7. Arrhenius plots for (a) Pd/a-SiO_2 and (b) Pd/f-SiO_2 catalysts.

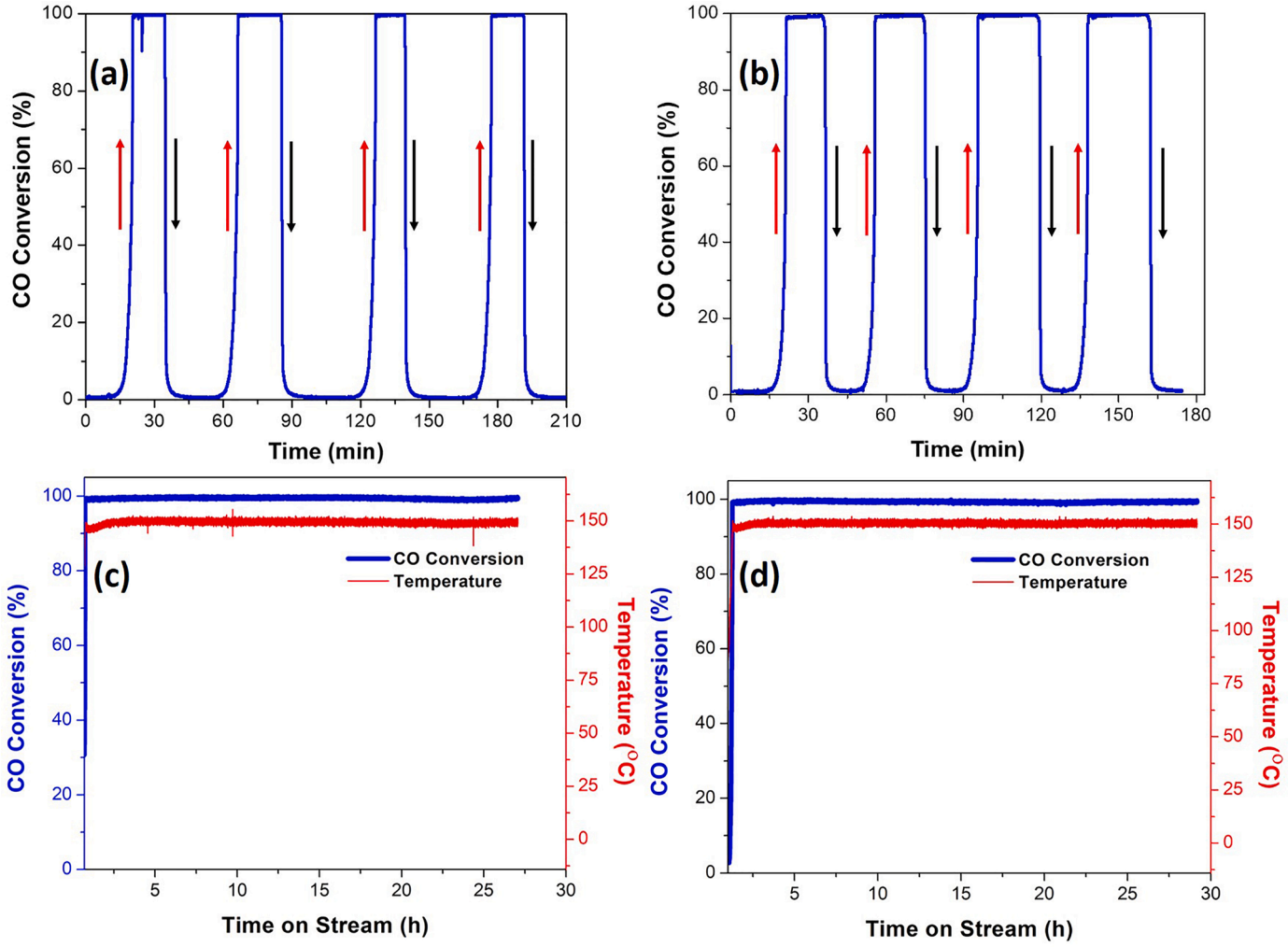

Fig. 8. Cyclic CO conversion percentage as a function of time of four heating and cooling cycles, and Long-term stability for Pd/a-SiO_2 (a) and (c) and for Pd/f-SiO_2 (b) and (d) catalysts catalytic activity experiment as a function of time in the stream, performed under a continuous flow of gas at 100% CO during the extinction cycle maintaining the temperature at 150 °C reaction temperature.

over palladium catalysts supported on silica aerogel to commercial fumed silica with 5% Pd loading. The two catalysts exhibited high catalytic performance and stability under the same conditions. XPS surface analysis and XRD results and confirms the presence of Pd^0. XPS also showed the presence of Pd^{2+} in Pd/a-SiO_2 and mainly Pd^0 and very small peaks of Pd^{2+}in Pd/f-SiO_2. All the peaks are slightly shifted to lower binding energies, suggesting a strong interaction between the silica support and Pd, where electrons transferred from Pd to the silica support indicating a strong metal-support interaction at the interface between Pd and Si, which can play a crucial role in the reaction dynamics.

Moreover, reaction parameters were found to play an important role in the CO oxidation reaction. The two catalysts showed different behaviors at different reaction parameters. Pd/a-SiO_2 catalyst was very sensitive to the catalyst weight, and the highest activity was achieved at 20 mg optimal catalyst weight compared to Pd/f-SiO_2, where the activity increased linearly with catalyst weight; the highest activity was achieved at 30 mg. CO conversion efficiency was better on Pd/a-SiO_2 at low flow rates (Laminar flow dominant), a 99.5% conversion was reached at an optimal flow rate of 100 cm^3/min, while Pd/f-SiO_2 showed better conversion at high flow rates (turbulence flow). Relative active sites were calculated from the pre-exponential factor in Arrhenius plots to support these results. Pd/a-SiO_2 has relative active sites ~x223C153, the apparent activation energy ~x223C88 kJ/mole, Pd/f-SiO_2 has ~x223C252, and the apparent activation energy ~x223C96 kJ/mole. Ignition-extinction hysteresis behavior was similar for both catalysts, where the hysteresis width shows sensitivity to catalyst weight and reached the largest width for 20 mg of catalyst, while it increases linearly with the ramp rate and flow rate. The maximum hysteresis width was obtained at 10 °C/min and 200 mL/min.

This study demonstrates that both catalysts have high catalytic activities and can be tuned by varying the surface, morphology, and reaction parameters and exhibit ignition-extinction conversion hysteresis and excellent catalytic stability CO oxidation reaction. The catalyst's surface, morphology, and porosity can influence the diffusion of reactants through the catalyst, the mass transfer, and active site accessibility. This study suggests that hysteresis is sensitive to thermal effects and mass transfer. Cyclic CO conversion and long-term stability tests confirm that both catalysts are recyclable and highly stable with the active sites' regeneration ability and maintain a full CO conversion without a decline in catalytic performance during the whole 27 h reaction time on stream.

CRediT authorship contribution statement

Rola Mohammad Al Soubaihi: Conceptualization, Methodology, Writing – original draft. **Khaled Mohammad Saoud:** Conceptualization, Methodology, Visualization, Investigation, Writing – review &

editing, Project administration. **Joydeep Dutta:** Conceptualization, Methodology, Supervision, Writing – review & editing, Project administration.

Declaration of Competing Interest

The authors declare that they have no known competing financial interests or personal relationships that could have appeared to influence the work reported in this paper.

References

[1] J. Gustafson, et al., The role of oxides in catalytic CO oxidation over rhodium and palladium, ACS Catal. 8 (5) (2018) 4438–4445.
[2] M.S. Chen, et al., Highly active surfaces for CO oxidation on Rh, Pd, and Pt, Surf. Sci. 601 (23) (2007) 5326–5331.
[3] J. Waikar, H. Pawar, P. More, Review on CO oxidation by noble and non-noble metal based catalyst.Catalysis in Green, Chemistry and Engineering 2 (2019) 11–24.
[4] S. Dey, et al., The choice of precursors in the synthesizing of CuMnOx catalysts for maximizing CO oxidation, Int. J. Ind. Chem. 9 (3) (2018) 199–214.
[5] M. Mokhtar, S.N. Basahel, Y.O. Al-Angary, Nanosized spinel oxide catalysts for CO-oxidation prepared via CoMnMgAl quaternary hydrotalcite route, J. Alloy. Compd. 493 (1) (2010) 376–384.
[6] M.R. Al Soubaihi, M.K. Saoud, J. Dutta, Critical review of low-temperature CO oxidation and hysteresis phenomenon on heterogeneous catalysts, Catalysts 8 (12) (2018).
[7] R.M. Al Soubaihi, et al., Synthesis of hierarchically porous silica aerogel supported palladium catalyst for low-temperature CO oxidation under ignition/extinction conditions, Microporous Mesoporous Mater. 292 (2020), 109758.
[8] E.M.C. Alayon, et al., On highly active partially oxidized platinum in carbon monoxide oxidation over supported platinum catalysts, J. Catal. 263 (2) (2009) 228–238.
[9] R. Sawisai, et al., Synthesis, characterization, and catalytic activity of Pd(II) salen-functionalized mesoporous silica, J. Chem. 2017 (2017) 1–12.
[10] Y. Xu, et al., CO oxidation over Pd catalysts supported on different supports: a consideration of oxygen storage capacity of catalyst, Adv. Mater. Res. 347-353 (2011) 3298–3301.
[11] K. Kosuge, P.S. Singh, Mixed-oxide pillared silicates from H-ilerite by intercalation, Chem. Mater. 12 (2) (2000) 421–427.
[12] N. Katabathini, I.H.A. El Maksod, M. Mokhtar, Cu, Fe and Mn oxides intercalated SiO_2 pillared magadiite and ilerite catalysts for NO decomposition, Appl. Catal. A 616 (2021), 118100.
[13] I. Yuranov, et al., Pd/SiO_2 catalysts: synthesis of Pd nanoparticles with the controlled size in mesoporous silicas, J. Mol. Catal. A Chem. 192 (1–2) (2003) 239–251.
[14] I. Miguel-García, et al., Capillary microreactors based on hierarchical SiO_2 monoliths incorporating noble metal nanoparticles for the preferential oxidation of CO, Chem. Eng. J. 275 (2015) 71–78.
[15] K.-i. Shimizu, et al., The average Pd oxidation state in Pd/SiO_2 quantified by L3-edge XANES analysis and its effects on catalytic activity for CO oxidation, Catal. Sci. Technol. 2 (4) (2012) 767.
[16] C. Cie, Color Management in Ink Jet printing, in Ink Jet Textile Printing. 2015, Elsevier. p. 43–57.
[17] J.S. Kwon, et al., The effect of support pretreatment with ammonia on Pd/SiO_2 catalyst, Mater. Sci. Forum 922 (2018) 125–129.
[18] Z.-.W. Kang, et al., Palladium supported on commercial fumed silica as sustainable catalyst for Suzuki-Miyaura coupling reactions, Silicon 11 (1) (2018) 287–292.
[19] J.B. Wang, S.C. Lin, T.J. Huang, Selective CO oxidation in rich hydrogen over CuO/samaria-doped ceria, Appl. Catal. A 232 (1–2) (2002) 107–120.
[20] K. Hauff, et al., Platinum oxide formation and reduction during NO oxidation on a diesel oxidation catalyst-experimental results, Appl. Catal. B 123-124 (2012) 107–116.
[21] Guy B. Marin, Gregory S. Yablonsky, Denis Constales. Kinetics of Chemical Reactions, Wiley-VCH Verlag GmbH & Co. KGaA, 2019.
[22] R.K. Dadi, D. Luss, V. Balakotaiah, Dynamic hysteresis in monolith reactors and hysteresis effects during co-oxidation of CO and C2H6, Chem. Eng. J. 297 (2016) 325–340.
[23] I. Koutoufaris, G. Koltsakis, Heat- and mass-transfer induced hysteresis effects during catalyst light-off testing, Can. J. Chem. Eng. 92 (9) (2014) 1561–1569.
[24] B. Heinrichs, et al., Cogelation: an effective sol-gel method to produce sinter-proof finely dispersed metal catalysts supported on highly porous oxides, in Studies in Surface Science and Catalysis, E. Gaigneaux, et al., Editors. 2000, Elsevier. p. 25–33.
[25] R. Raj, M.P. Harold, V. Balakotaiah, Steady-state and dynamic hysteresis effects during lean co-oxidation of CO and C_3H_6 over Pt/Al_2O_3 monolithic catalyst, Chem. Eng. J. 281 (2015) 322–333.
[26] J.W Geus, A.J van Dillen, Preparation of supported catalysts by deposition-precipitation. Preparation of Solid Catalysts, Wiley-VCH Verlag GmbH, 2022, pp. 460–487.
[27] vol I, . Edited by A. Taylor, D. Briggs, M.P. Seah, Practical Surface Analysis by Auger and X-ray Photoelectron Spectroscopy, 2nd ed., John Wiley, New York, 1990, p. 657. vol I, . Edited bypp., price: £86.50. ISBN 0471 92081 9. Journal of Chemical Technology & Biotechnology, 2007. **53**(2): p. 215-215.
[28] R.M. Al Soubaihi, et al., CO oxidation efficiency and hysteresis behavior over mesoporous Pd/SiO_2 catalyst, Catalysts 11 (1) (2021) 131.
[29] K.S. Abdel Halim, et al., Factors affecting CO oxidation over nanosized Fe_2O_3, Mater. Res. Bull., 42 (4) (2007) 731–741.
[30] P.A. Carlsson, M. Skoglundh, Low-temperature oxidation of carbon monoxide and methane over alumina and ceria supported platinum catalysts, Appl. Catal. B 101 (3–4) (2011) 669–675.
[31] N.K. Soliman, Factors affecting CO oxidation reaction over nanosized materials: a review, J. Mater. Res. Technol. 8 (2) (2019) 2395–2407.
[32] N.Y. Usachev, et al., Hysteresis phenomenon in CO and hydrogen oxidation on Cu-Ce-Zr-O systems, Mendeleev Commun. 14 (2) (2004) 79–80.
[33] A. Bertoluzza, et al., Raman and infrared spectra on silica gel evolving toward glass, J. Non Cryst. Solids 48 (1) (1982) 117–128.
[34] G. Li, et al., Preparation of Cu-SiO_2 composite aerogel by ambient drying and the influence of synthesizing conditions on the structure of the aerogel, Chin. Sci. Bull. 56 (7) (2011) 685–690.
[35] J.D. Riley, et al., Partial densities of states in amorphousPd0.81Si0.19, Phys. Rev. B 20 (2) (1979) 776–783.
[36] E.V. Monteiro, H. Varela, R.B. Faria, The effect of flow rate on the oscillatory activation energy of an oscillating reaction, Chem. Phys. Lett. 684 (2017) 219–224.
[37] X. Sun, et al., Effects of reaction temperature and inlet oxidizing gas flow rate on IG-110 graphite oxidation used in HTR-PM, J. Nucl. Sci. Technol. 54 (2) (2016) 196–204.
[38] M. Berdau, et al., Kinetic phase diagram for CO oxidation on Pt(210): pattern formation in the hysteresis and oscillation regions, J. Chem. Phys. 106 (10) (1997) 4291–4308.
[39] Z. Wang, et al., Size and support effects for CO oxidation on supported Pd catalysts, Sci. China Chem. 53 (9) (2010) 2047–2056.
[40] C.I. Contescu, et al., Practical aspects for characterizing air oxidation of graphite, J. Nucl. Mater. 381 (1–2) (2008) 15–24.